

Studies and evaluations on interception processes during rainfall based on a tank model

Michio Hashino*, Huaxia Yao, Hiromu Yoshida

Department of Civil Engineering, The University of Tokushima, 2-1 Minami-josanjima, Tokushima 770-8506, Japan

Received 25 July 2000; revised 18 July 2001; accepted 19 July 2001

Abstract

Some analyses are carried out with regard to canopy interception processes during rainfall events based on a tank model. A hypothesis, rainfall interception rate is proportional to the product of potential evaporation and rainfall intensity, is formed from past experimental data, and is applied to the data in this study. Computational equations are proposed to the interception rate and accumulative interception loss under constant rainfall intensity. Data from the Shirakawatani experimental forested catchment are used in order to examine the relationship between the interception rate and rainfall intensity, the ratio of the interception rate to rainfall intensity and potential evaporation, accumulative interception loss and the rainfall duration, and accumulative interception loss and accumulative rainfall. These regression relations show that interception processes are described by rainfall intensity and potential evaporation. An equation relating the aerodynamic resistance in the Penman–Monteith equation to rainfall intensity is proposed to explain the fact that the interception rate exceeds net radiation. © 2002 Elsevier Science B.V. All rights reserved.

Keywords: Analysis; Forest canopy; Interception; Evaporation; Rainfall; Regression

1. Introduction

Gross rainfall on a canopy is classified into rainfall interception loss, throughfall, and stemflow. Rainfall interception loss is defined as the residual after subtracting throughfall and stemflow from gross rainfall. A lot of data for forested catchments with different types of trees and climatic conditions have been collected by field observations in the world (e.g. Horton, 1919; Rutter et al., 1971, 1975; Gash, 1979). For various kinds of forest stands, a linear relation between the interception loss and gross rainfall

during a rainfall event results in

$$I = aR + b \quad (1.1)$$

where I is the interception loss, R the rainfall in a rainfall event, and a and b are empirical constants.

aR of Eq. (1.1) stands for the rainfall that evaporates during raining periods; b indicates intercepted rainwater which still remains on leaves and branches when the rain stops after the raining periods. Constant b usually is 1.3–2.0 mm for conifers (Horton, 1919; Rutter et al., 1971; Rutter et al., 1975; Gash, 1979; Tsukamoto et al., 1988) and constant a is 0.13–0.26 being approximately the ratio of interception loss to gross rainfall during a raining event. As a result, there will be an interception loss of 26.0–52.0 mm when heavy rainfall of 200.0 mm occurs. This is partly the

* Corresponding author. Fax: +81-88-65-67-332.

E-mail address: michio@ce.tokushima-u.ac.jp (M. Hashino).

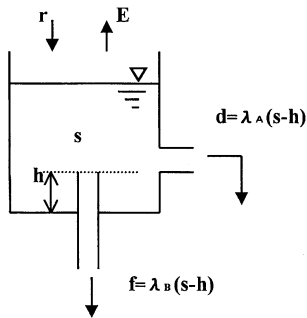


Fig. 1. Tank model.

reason for floods becoming smaller in forested catchments than the ones in unforested catchments.

Gash (1979) showed that the empirical constant a in Eq. (1.1) is in the ratio of the average interception rate \bar{e} to the average rainfall intensity \bar{r} during the raining periods as given below:

$$a = \frac{\bar{e}}{\bar{r}} \quad (1.2)$$

Tsukamoto et al. (1988) obtained satisfactory data of hourly interception loss using the 'single-tree monitoring device', and demonstrated the applicability of Eq. (1.2) for a range of $1 < r < 7$ mm/h. However, it is rather doubtful whether Eq. (1.2) can or cannot be applied if rainfall intensity exceeds 10 mm/h. According to the above statement, the interception rate is proportional to the rainfall intensity. The relations of the interception loss to the other micrometeorological factors are unknown. Klaassen et al. (1998) showed that the relation between interception loss and rainfall intensity is exponential. Schulze et al. (1978) also pointed out that interception increases with rainfall intensity for given durations of a storm.

It is important to physically and separately describe evaporation of intercepted rainwater during rainfall events and transpiration between rainfall events in

order to analyze water circulation, flood formation, and low flow processes in forested catchments (Hashino et al., 1999). These are two quite different primary processes in water circulation. Hashino et al. (1989) has been collecting field data from an experimental forested catchment since 1985. Rainfall interception experiments were carried out with one tree in a big hall, and a mathematical model based on a tank model was proposed. Furthermore, the model was verified with in situ data (Hashino et al., 1991, 1992). A more detailed introduction on the model was provided by Yoshida and Hashino (1994). According to the above-mentioned model, the evaporation rate E shown in Eq. (1.3)

$$E = \alpha^* E_p s / h \quad (1.3)$$

describes the rainfall interception phenomena, i.e. the relation between rainfall interception loss and gross rainfall. Here E is the evaporation rate from the water of the canopy tank, E_p the potential evaporation rate evaluated by the Penman equation, s the water storage of the canopy tank, h the water capacity after the rainfall, and α^* a parameter. However, the evaporation rate E by Eq. (1.3) is difficult to be applied because the hourly data are necessary to evaluate the water storage of canopy s in Eq. (1.3).

It was shown that the evaporation rate E could be expressed by Eq. (1.4) with a simple canopy tank model (seeing Fig. 1) under the following conditions: (a) without stem tank, (b) h is supposed to be zero, (c) steady state of the canopy storage, and (d) constant rainfall intensity. The evaporation rate E is derived from a canopy tank model taking h into account (Yulianur et al., 1998):

$$E = CE_p r \text{ or } \frac{E}{r} = CE_p \quad (1.4)$$

Coefficient C is determined by the state of the forest (type and age of tree). The trees in the experimental forest are 30 years old Sugi (*Cryptomeria japonica*), values of coefficient C are about 1.73 h/mm for rainfall events, and 1.6–2.1 h/mm for hourly rainfall-interception analysis (referring to Tables 1 and 2). In Eq. (1.2) taken from Gash, the interception ratio a does not change with time, while in Eq. (1.4), the ratio changes with time and is affected by meteorological parameters: temperature, humidity, wind speed, and radiation.

Table 1
Regressions of interception to selected variables

Variable	Regression	CC
With potential evaporation E_p	$\bar{i} = 9.511\bar{E}_p - 0.269$	0.342
With rainfall rate r	$\bar{i} = 0.226\bar{r} - 0.028$	0.847
With product of r and E_p	$\bar{i} = 1.758\bar{E}_p\bar{r} - 0.073$	0.903

Table 2
Regressions of accumulative interception to time duration

Situation for total interception		CC
Having potential evaporation E_p	$I = 5.869\bar{E}_p T_r + 1.748$	0.760
Having rainfall rate r	$I = 0.231\bar{r} T_r - 1.538$	0.868
Having product of r and E_p	$I = 1.503\bar{E}_p \bar{r} T_r + 3.139$	0.886
Situation for accumulative interception		
Having potential evaporation E_p	$I = 7.92\bar{E}_p(t - 20) + 0.032$	0.816
Having rainfall rate r	$I = 0.316\bar{r}(t - 20) - 4.024$	0.965
Having product of r and E_p	$I = 1.89\bar{E}_p \bar{r}(t - 20) - 1.758$	0.975

Based on the experience and achievements mentioned above, theoretical and analytical analyses are made in this study. These analyses are designed separately for interception processes under constant rainfall, time series of accumulative interception under constant rainfall, and the relationship of accumulative interception to accumulative rainfall.

Using the data obtained from the Shirakawatani experimental forested catchment and other study areas, the interception processes are investigated by the following relations: (1) interception rate to rainfall intensity, (2) average interception ratio in a rainfall event to rainfall duration, (3) total interception loss to rainfall duration, and (4) total interception loss to gross rainfall. Finally, the relation of aerodynamic resistance in the Penman–Monteith equation to rainfall intensity is classified.

The Shirakawatani experimental catchment is located in the western Tokushima Prefecture, Shikoku Island, Japan, having an area of 23 ha, altitude of 740–1140 m, and an average slope of 21.5°. Three fifth of the catchment is covered by *Cryptomeria japonica* (21–36 years old) and the remainder is covered with broad-leaf trees (27–31 years old). The stand is on a brown forest soil. Rainfall, throughfall, stemflow, air temperature, relative humidity, wind speed and net radiation are observed.

2. Theoretical derivations

The water circulation processes on the trees are simulated according to a ‘rainfall interception tank model’ (Hashino et al., 1989; Yoshida et al., 1993). Interception rate and its relation to rainfall intensity and other variables will be discussed later.

2.1. Description of interception rate during raining periods

Fig. 1 shows the tank model (referring to Yoshida and Hashino, 1994). The parameter h of the storage capacity of the canopy is supposed not to change during the rainfall events. Evaporation from the stems is presumed negligible. At arbitrary time t during the raining periods, the water balance equation for the canopy tank is quoted as follows:

$$\frac{ds}{dt} = r - d - E - f \quad (2.1)$$

where s is the depth of water storage (mm) in the tank, r , the rainfall intensity (mm/h), d , the drip rate (mm/h), f , the stemflow rate (mm/h), and E , the evaporation rate from the tank (mm/h). Both drip and stemflow are described as a function of s .

$$d = 0 \quad f = 0 \quad (0 \leq s \leq h) \quad (2.2)$$

$$d = \lambda_A(s - h) \quad f = \lambda_B(s - h) \quad (s > h) \quad (2.3)$$

where λ_A and λ_B are parameters for drip and stemflow. As an example, Yoshida and Hashino (1994) once got the values of parameters for an experimental forest: $\lambda_A = 2.44 \text{ h}^{-1}$, $\lambda_B = 2.38 \text{ h}^{-1}$, and $h = 1.36 \text{ mm}$.

Evaporation rate E is described as a product of potential evaporation E_p and the depth of water storage s as mentioned above

$$E = \alpha^* E_p s / h = \alpha s \quad (2.4)$$

E_p is evaluated by the Penman equation with micro-meteorological data; α is defined by the after-mentioned equation:

$$\alpha = \alpha^* E_p / h \quad (2.5)$$

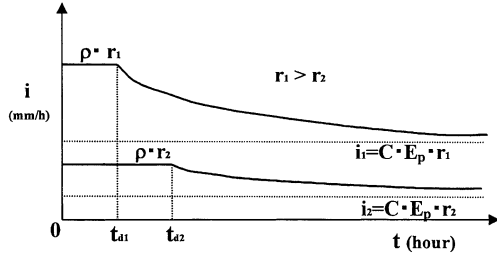


Fig. 2. Interception rate i and elapsed time t .

On the other hand, the interception rate i (mm/h) is defined as the sum of evaporation and water storage change of canopy during a short time (an hour for example). From Eq. (2.1) the interception rate can be described as the subtraction of throughfall and stemflow from rainfall intensity:

$$i = r - [(1 - \rho)r + \rho d] - \rho f = \rho r - \rho d - \rho f \quad (2.6)$$

where ρ is the ratio of the projective area of the canopy to the ground. Substituting Eq. (2.6) for Eq. (2.1), a relation between interception rate i and evaporation rate E is obtained:

$$i = \rho E + \rho \frac{ds}{dt} \quad (2.7)$$

Under the steady condition, namely, $ds/dt = 0$, i is equal to ρE .

2.2. Evaporation rate under constant rainfall

The depth of water storage s is obtained as follows: Eqs. (2.2), (2.3), and (2.4) are substituted for Eq. (2.1), and Eq. (2.1) is integrated by t under the initial condition of $s = 0$ at $t = 0$. In that case α is presumed constant. The resulted equations are written as

$$s = r(1 - e^{-\alpha t})/\alpha \quad (0 \leq t \leq t_d \text{ or } 0 \leq s \leq h) \quad (2.8)$$

$$s = h + (r - \alpha h)[1 - e^{-(\alpha + \lambda)(t - t_d)}]/(\alpha + \lambda) \quad (t > t_d \text{ or } s > h) \quad (2.9)$$

where $\lambda = \lambda_A + \lambda_B$ and t_d is the time when drip and stemflow begin.

Substituting Eqs. (2.6), (2.8) and (2.9) for Eq. (2.7)

yields to

$$i = \rho r \quad (0 \leq t \leq t_d \text{ or } 0 \leq s \leq h) \quad (2.10)$$

$$i = \rho \{ \alpha(r + \alpha h) + \lambda(r - \alpha h) \exp[-(\alpha + \lambda) \times (t - t_d)] \} / (\alpha + \lambda) \quad (t > t_d \text{ or } s > h) \quad (2.11)$$

After sufficient time has passed, interception processes will reach an equilibrium state. The interception rate i is given in Eq. (2.12) by substituting an infinity of t in Eq. (2.11):

$$i^* = \rho \alpha (r + \alpha h) / (\alpha + \lambda) \quad (2.12)$$

The fact that $\lambda \gg \alpha$ was confirmed by the data obtained in the Shirakawatani catchment (Yoshida et al., 1993). Substituting Eq. (2.5) for Eq. (2.12) leads to

$$\begin{aligned} i^* &= \frac{\rho \alpha (r + \alpha h)}{\alpha + \lambda} = \rho \frac{\alpha}{\lambda} \frac{r + \alpha h}{1 + \frac{\alpha}{\lambda}} \approx \rho \frac{\alpha}{\lambda} (r + \alpha h) \\ &= \rho \frac{\alpha^* E_p}{\lambda h} \left(r + \frac{\alpha^* E_p}{h} h \right) = \rho \frac{\alpha^* E_p r}{\lambda h} \left(1 + \frac{\alpha^* E_p}{r} \right) \\ &\approx \frac{\rho \alpha^*}{\lambda h} E_p r = C E_p r \end{aligned} \quad (2.13)$$

where $C (= \rho \alpha^* / (\lambda h))$ is a parameter mainly determined by the type of tree and canopy state, although it is affected by micrometeorological conditions around the canopy. Eq. (2.13) shows that the interception rate is approximately proportional to the product of potential evaporation E_p and rainfall intensity r .

Interception processes under constant rainfall are as follows: The interception rate is constant, i.e. $i = \rho r$ before drip and stemflow begin. After that the interception rate gradually approaches an asymptotic line ($i^* = C E_p r$) as shown in Fig. 2. A typical characteristic of the proposed method is that the interception rate is not only related to potential evaporation but also to rainfall intensity. The concept also proved applicable according to experimental results (Yoshida et al., 1993; Yulianur et al., 1998).

As a result, the ratio of the interception rate to rainfall intensity is obtained according to Eq. (2.13) and is proportional to potential evaporation:

$$\frac{i^*}{r} = C E_p \quad (2.14)$$

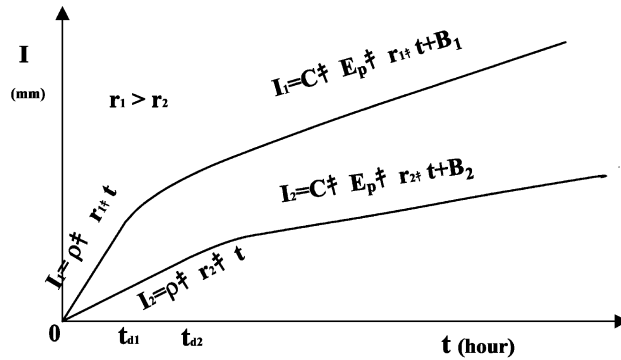


Fig. 3. Accumulative interception loss I and elapsed time t .

The ratio on summer days is higher than on winter days if the rainfall intensity remains unchanged. There are two possible reasons for this difference. Coefficient C reflects partly structure of forest trees and the canopy area of trees changes seasonally. The canopy has more leaf area and is more active in summer than in winter. Temperature and potential evaporation also change from summer to winter.

2.3. Accumulative interception loss under constant rainfall

When integrating Eqs. (2.10) and (2.11), accumulative interception loss at time t can be obtained analytically.

$$I = \int_0^t \rho r dt = \rho r t \quad (0 \leq t \leq t_d) \tag{2.15}$$

$$I = \rho h +$$

$$\int_{t_d}^t \rho [\alpha(r + \alpha h) + \lambda(r - \alpha h)e^{-(\alpha + \lambda)(t - t_d)}] / (\alpha + \lambda) dt$$

$$= B + i^* t - \frac{\rho \lambda (r - \alpha h)}{(\alpha + \lambda)^2} e^{-(\alpha + \lambda)(t - t_d)} \quad (t > t_d) \tag{2.16a}$$

in which

$$i^* = \frac{\rho \alpha (r + \alpha h)}{\alpha + \lambda}$$

$$B = \rho h - \frac{\rho \alpha h (r + \alpha h)}{(\alpha + \lambda) r} + \frac{\rho \lambda (r - \alpha h)}{(\alpha + \lambda)^2} \tag{2.16b}$$

where I is the accumulative interception loss, i^* and B

are constant coefficients. If the rainfall intensity increases, i^* and B will also do so.

Furthermore, an asymptotic line can be defined as

$$I^* = i^* t + B \approx C E_p r t + B \tag{2.17}$$

whereas parameter C is defined in Eq. (2.13). Therefore, parameter B is the intercept of the asymptotic line and parameter i^* is the gradient of the asymptotic line becoming steeper with rainfall intensity. The curves of accumulative interception versus time is shown in Fig. 3.

2.4. Relation between accumulative interception loss and accumulative rainfall

If accumulative rainfall at time t is written as R , replacing t by $t = R/r$ or $t - t_d = (R - h)/r$ in Eqs. (2.15) and (2.16a) shows the relation of accumulative interception loss to rainfall.

$$I = \rho R \quad (0 \leq t \leq t_d) \tag{2.18}$$

$$I = B + \frac{i^*}{r} R - \frac{\rho \lambda (r - \alpha h)}{(\alpha + \lambda)^2} e^{-((\alpha + \lambda)/r)(R - h)} \quad (t > t_d) \tag{2.19}$$

where $I^* = i^*/r R + B$ is the asymptotic line of the accumulative interception loss, and gradient i^*/r , i.e. the ratio of interception loss to rainfall in a rainfall event (I/R) is affected by potential evaporation as shown in Eq. (2.14). The relations are demonstrated in Fig. 4.

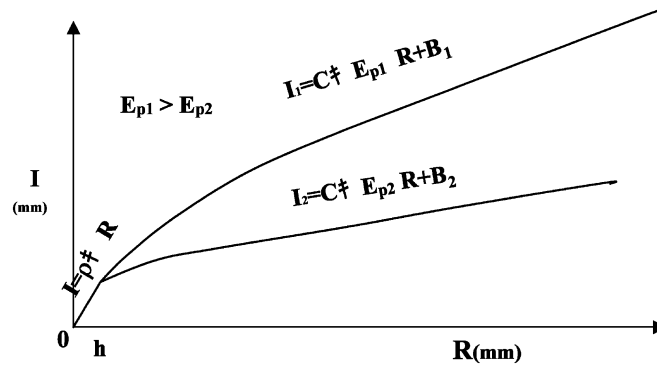


Fig. 4. Accumulative interception loss I and total rainfall R .

3. Verification of the theories by field data

3.1. Relation between interception and rainfall intensity

Tsukamoto et al. (1988) measured the hourly mean value of interception rate E of a single tree in a forest, and found that the interception rate was proportional to rainfall intensity r when the rainfall intensity was less than 7.0 mm/h. Yoshida et al. (1993) evaluated hourly and total interception loss in a rainfall event using the authors' tank model, and found that the mean value of the interception rate in a rainfall event was proportional to average rainfall intensity. Pearce and Rowe (1981) pointed out that the ratio of the average interception rate to average rainfall intensity in a rainfall event was around 0.29 ($r = 1.58$ mm/h, $i = 0.46$ mm/h) in summer, while in winter it was 0.18 ($r = 1.55$ mm/h

$i = 0.28$ mm/h), i.e. much less than in summer. Yulianur et al. (1998) classified the data of total interception loss and average rainfall intensity of rainfall events into two groups: temperatures θ less than 10°C and higher than 20°C , and correlated them. They found that the regression coefficient $a = E/r$ in the case of $\theta > 20^\circ\text{C}$ is 1.7 times larger than that in the case of $\theta < 10^\circ\text{C}$. These facts prove that the interception rate could be well explained by potential evaporation and rainfall intensity, i.e. $i^* = CE_p r$, but not satisfactorily by potential evaporation ($i^* = CE_p$).

Data from the Shirakawatani catchment (1991–1996) are used for verifying the hypotheses and theories mentioned above. Average rainfall intensity and interception rate of all events (91 rainfall events) are shown in Fig. 5. The figure shows that interception rate i during raining periods is closely related to rainfall intensity. The fact that interception rate may reach 10 mm/h is remarkably noticed. A rainfall event is defined as a rainy period with dry periods of less than 6 h and a dry period before and after the rainfall event of at least 12 h.

The regression equations are shown in Table 1. Average interception rate has a certain correlation to rainfall intensity. for all 91 rainfall events, Correlation coefficients (CCs) for the 91 rainfall events are also listed in Table 1.

The correlation of the interception rate with potential evaporation is very low, and the extraordinary value of parameter such as 9.511 cannot be explained physically. The correlation of the interception rate with rainfall intensity is high, with the product of potential evaporation and rainfall intensity even higher. In other words, the results show that

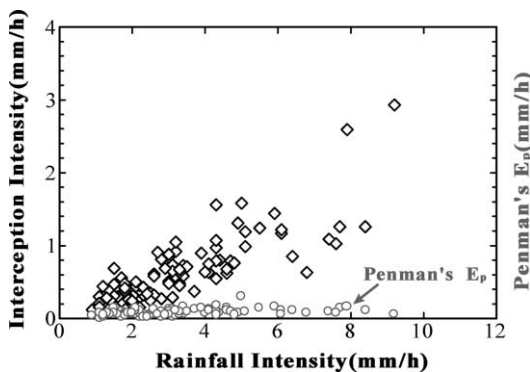


Fig. 5. Average interception rate I and rainfall intensity r in rainfall events.

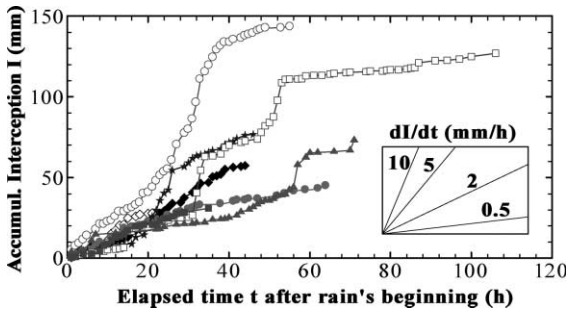


Fig. 6. Accumulative interception loss I and elapsed time t .

the interception rate cannot be described by potential evaporation only.

3.2. Relations between accumulative interception loss and rainfall duration

Schulze et al. (1978) made a regression analysis on accumulative interception loss I and rainfall duration T_r classifying rainfall intensity into four groups: 0.0–1.4, 1.5–2.9, 3.0–5.9 and >6.0 mm/h. They found that interception loss increased with rainfall intensity when the rainfall duration lasted equally long. Hattori et al. (1982) and Yoshida et al. (1993) carried out analyses similar to that of Schulze. They came to the same conclusions.

Based on these experimental facts, accumulative loss cannot be described by potential evaporation only, but can be described by both rainfall intensity and potential evaporation as shown in Eqs. (2.16a) and (2.17).

Eight different rainfall events were chosen in the Shirakawatani catchment of which total rainfall and rainfall duration were over 150 mm and longer than

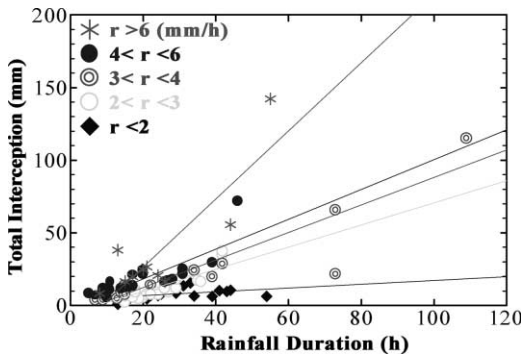


Fig. 7. Total interception loss of rainfall event and rainfall duration.

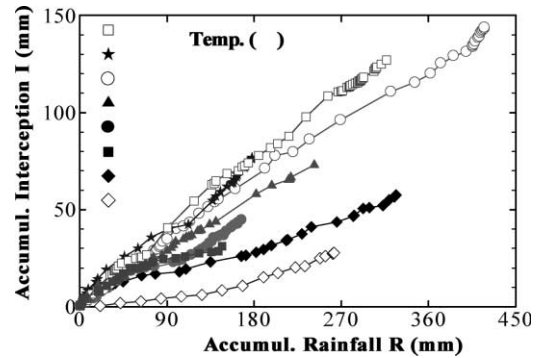


Fig. 8. Accumulative interception loss and rainfall at elapsed time.

20 h, respectively. The relation between the accumulative interception loss I and the elapsed time t are plotted in Fig. 6, with each line representing a rainfall event. Apparently, intensive interception rate is observed (some mm/h to 10 mm/h), even after 20 h.

Total interception loss of a rainfall event and rainfall duration are plotted in Fig. 7, and separated by rainfall intensities. It is apparent that total interception loss increases with rainfall duration and intensity.

The results of regression analysis among total interception loss, potential evaporation, and rainfall duration are shown in Table 2. Two situations are considered: (1) total interception loss of a rainfall event with 91 samples; (2) accumulative interception loss at arbitrary time during the heavy rainfall events with 745 samples. The effect of average potential evaporation E_p , average rainfall r and average $E_p r$ on the CC is considered. The CC proves to be largest when both potential evaporation and rainfall intensity are considered in either situation. The suggested Eqs. (2.16a) and (2.17) prove to be acceptable.

3.3. Relations between accumulative interception loss and total rainfall

The relation between accumulative interception loss and total rainfall of the above-mentioned eight rainfall events at different temperature is shown in Fig. 8. The accumulative interception loss in a rainfall event increases linearly with total rainfall, and the gradient becomes steeper when temperature rises.

Total interception loss and rainfall during a rainfall event is shown in Fig. 9. These figures confirmed the applicability of Eq. (2.19), i.e. $I^* = CE_p R + B$.

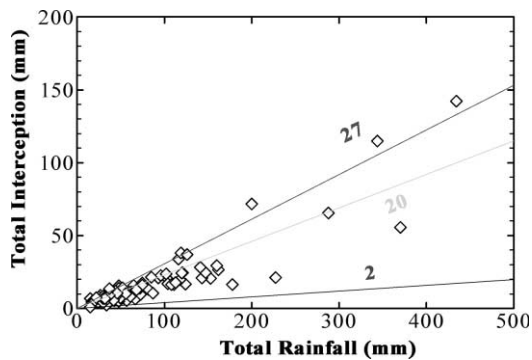


Fig. 9. Total interception loss and rainfall of rainfall event.

The field data used in Table 2 are also applied to obtain regression relations of accumulative interception loss to total rainfall. The results are listed in Table 3. The product of total rainfall and potential evaporation results in the most satisfactory CC.

The results obtained are summarized as follows: interception processes cannot be described by the hypothesis of $E = CE_p$, i.e. evaporation rate from canopy is proportional only to potential evaporation. However, Eq. (1.4), i.e. $E = CE_p r$ recommended in this study describes the above results satisfactorily. Thus, the interception rate is proportional to both rainfall intensity and potential evaporation. The suggested theory has been examined by field data obtained in the Shirakawatani catchment.

4. Relation between aerodynamic resistance in the Penman–Monteith equation and rainfall intensity

Stewart (1977), Hattori et al. (1981, 1982), Hattori (1985), and Lindroth (1985) reported that the evapora-

tion rate from wet canopy was higher than the one from dry canopy under the same radiation, and the evaporation rate from wet canopy sometimes exceeds effective or net radiation, and is higher several times than the above-mentioned radiation. Hattori (1985) observed interception loss and meteorological parameters in forests. He identified the parameters in the Penman–Monteith equation and the Rutter model, and obtained hourly interception rates in a range of 0.0–0.8 mm/h. The interception rates above 0.2 mm/h almost exceeded the effective radiation. As a result, the ratio of sensible heat to latent heat becomes minus. Mizutani and Ikeda (1994) also reported a negative sensible heat during rain events. However, the ratio should not become negative, if the vertical energy balance was correct. Thus, these results show that the horizontal heat exchange is not negligible.

Rainfall events lasting longer than 20 h are collected in the Shirakawatani catchment. Average and standard deviation of hourly net radiation (unit of mm/h), Penman potential evaporation, interception rate, and rainfall intensity are listed in Table 4. CCs of interception rate to other items are also listed.

The average interception rate is higher than the average net radiation and Penman potential evaporation. The interception rate is correlated closest to rainfall intensity.

The result that the interception rate exceeds net radiation has never been confirmed or interpreted by the traditional theories based on vertical energy balance. It is thought that a horizontal heat advection result in or contribute to the strange phenomenon, and this advection or heat transfer should be connected with wind and aerodynamic process. Therefore in this paper, the Penman–Monteith equation is considered to estimate interception evaporation, and some

Table 3
Regressions of accumulative interception to rainfall

Situation for total interception		CC
Only potential evaporation E_p	$I = 5.869\bar{E}_p/\bar{r}R + 1.748$	0.760
Only rainfall R	$I = 0.231R - 1.538$	0.868
Product of R and E_p	$I = 1.508\bar{E}_pR + 3.172$	0.888
Situation for accumulative interception		
Only potential evaporation E_p	$I = 7.92\bar{E}_p/\bar{r}(R - R_{20}) + 0.032$	0.816
Only rainfall R	$I = 0.316(R - R_{20}) - 4.024$	0.965
Product of R and E_p	$I = 1.894\bar{E}_p(R - R_{20}) - 1.798$	0.975

Table 4
Averages and variations of interception, rainfall rate and potential evaporation (mm/h)

	Interception	Rainfall	Net radiation	Penman E_p
Average (mm/h)	0.71	3.30	0.20	0.16
Standard deviation (mm/h)	1.38	5.04	0.17	0.12
CC		0.834	0.000	0.000

efforts are made to try to explain the phenomenon of the extensive interception rate during rains. The Penman–Monteith equation for a wet canopy (the surface resistance or stomatal resistance for wet leaves is negligible) is written as

$$\lambda E_M = \frac{\Delta}{\Delta + \gamma} (R_N - G) + \frac{\rho_a C_p [e_s(\theta) - e_a]}{(\Delta + \gamma) r_a} \quad (4.1)$$

in which E_M is the evaporation rate (in unit of kg/s m^2) from the wet canopy surface, λ the vaporation constant (J/kg), R_N the net radiation (J/s m^2), G the heat transfer (J/h m^2) into ground soil, ρ_a the air density (kg/m^3), C_p the specific heat constant of air (J/kg K), $e_s(\theta)$ the saturated vapor pressure (hPa) for air temperature θ (K), e_a the vapor pressure (hPa), r_a the aerodynamic resistance (s/m), Δ , the gradient of saturated vapor pressure versus temperature (hPa K^{-1}), and γ , the psychrometer constant (hPa K^{-1}).

The aerodynamic resistance r_a is one of the most important parameters related to evaporation E_M during rainfall. The interception rate (i^*) during rains can be thought to be equal to the evaporation rate (E_M). The interception rate is estimated by Eq. (2.13). Therefore, combining Eq. (4.1) for E_M and Eq. (2.13) for i^* yields the following relation:

$$r_a = \frac{\rho_a C_p [e_s(\theta) - e_a]}{(\Delta + \gamma) \lambda C E_p r - \Delta (R_N - G)} \quad (4.2)$$

Substituting the Penman equation of potential evaporation (4.3) for Eq. (4.2)

$$\lambda E_p = \frac{\Delta}{\Delta + \gamma} (R_N - G) + \frac{\gamma}{\Delta + \gamma} f(u) [e_s(\theta) - e_a] \quad (4.3)$$

where $f(u)$ is an empirical function of wind speed u .

The following relation is obtained:

$$r_a = \frac{\rho_a C_p [e_s(\theta) - e_a]}{\Delta (R_N - G) (Cr - 1) + \gamma f(u) Cr [e_s(\theta) - e_a]} \quad (4.4)$$

This relation shows that the resistance during rainfall is related to the radiation $R_N - G$, deficit vapor pressure $e_s(\theta) - e_a$, wind speed u , and rainfall intensity r . When the rainfall intensity increases, the resistance will decrease, and then evaporation will get intensive. This relation partly explains the occurrence of extraordinary values of interception rate exceeding the effective radiation, although exact theoretical interpretation still needs further research.

Defining the special resistance in the case of $i = E_p = (R_N - G)/\lambda$ as r_{ac} , and r_{ac} is obtained by substituting $Cr = 1$ for Eq. (4.4):

$$r_{ac} = \frac{\rho_a C_p}{\gamma f(u)} \quad (4.5)$$

A non-dimensional resistance is obtained from Eqs. (4.4) and (4.5):

$$\frac{r_a}{r_{ac}} = \frac{1}{\frac{\Delta (R_N - G)}{\gamma f(u) [e_s(\theta) - e_a]} (Cr - 1) + Cr} \quad (4.6)$$

If there occurs horizontal heat transfer, it produces additional evaporation, i.e.

$Cr = i/E_p > 1$; the ratio r_a/r_{ac} is less than 1 as defined in Eq. (4.6). Usually, the horizontal heat advection occurs during rain, which results in a large value for Cr resulting in a large value for r_a (maybe much larger than r_{ac}). This will produce a small resistance and a big evaporation rate.

5. Concluding remarks

The authors had already reported that the evaporation

E from intercepted water was proportional to the product of potential evaporation E_p and interception water storage s . However, the relation between evaporation and rainfall intensity and meteorological parameters had not been clarified yet. In this research, the relations between interception rate and both rainfall intensity and potential evaporation were derived from a canopy tank model, which takes water storage on canopy into consideration. Interception rate i is proportional to the product of rainfall intensity r and potential evaporation E_p . The relation of accumulative interception loss I in a rainfall event to rainfall duration T_r is dominated by the average rainfall intensity, the relation of accumulative interception loss to the total rainfall is affected by the average temperature, i.e. potential evaporation during raining periods.

The above-mentioned results were tested with field data from the Shirakawatani experimental forested catchment. The extraordinarily high interception rate during heavy rainfall events cannot be described by the vertical energy balance. The proposed expression of aerodynamic resistance used in the Penman–Monteith equation, by including the rainfall intensity, might partly explain this phenomenon.

This study shows that the horizontal heat transport might be an important contribution to the interception rate during rains, and this contribution should not be neglected.

Acknowledgements

This study is partially supported by a Grant-in-Aid for Scientific Research, the Ministry of Education, Science, Sports and Culture, Japan (No. 12650516). Thanks are given to Margret Moussa for a careful review of the manuscript and constructive suggestions. The authors gratefully appreciate the valuable comments and suggestions of the anonymous reviewers.

References

- Gash, J.H.C., 1979. A analytical model of rainfall interception by forests. *Q. J. R. Meteorol. Soc.* 105, 43–55.
- Hashino, M., Yoshida, H., Takahashi, M., 1989. Comparison of rainfall interception models. Proceedings of 1989 Annual Conference. *Jpn Soc. Hydrol. Water Resour.*, Tokyo, 13–16 in Japanese.
- Hashino, M., Yoshida, H., Nakatani, T., Kimura, M., 1991. Conceptualization of evaporation in rainfall-interception model. Proceedings of 1991 Annual Conference. *Jpn Soc. Hydrol. Water Resour.*, Tokyo, 30–33 in Japanese.
- Hashino, M., Yoshida, H., Kimura, M., Nakatani, T., 1992. Analysis of canopy evaporation using a interception model. Proceedings of 1992 Annual Conference. *Jpn Soc. Hydrol. Water Resour.*, Tokyo 1992, 168–171 in Japanese.
- Hashino, M., Yao, H., Yoshida, H., 1999. Separation of rainfall interception and transpiration from annual evapotranspiration in forested watersheds. *Annu. J. Hydraul. Engng, JSCE* 43, 73–78.
- Hattori, S., 1985. Energy-balance characteristics of canopy interception. *J. Jpn. For. Soc.*, 358–365 in Japanese, with English Abstract.
- Hattori, S., Chikaarashi, H., Takeuchi, N., 1981. Estimation of evapotranspiration from a Hinoki stand using the energy balance method. *J. Jpn. For. Soc.* 63, 125–132 in Japanese, with English Abstract.
- Hattori, S., Chikaarashi, H., Takeuchi, N., 1982. Measurement of the rainfall interception and its micrometeorological analysis in a Hinoki stand. *Bull. For. For. Prod. Res. Inst.* 318, 79–102 in Japanese.
- Horton, R.H., 1919. Rainfall interception. *Mon. Wea. Rev.* 47, 603–623.
- Klaassen, W., Bosveld, F., Water, E.D., 1998. Water storage and evaporation as constituents of rainfall interception. *J. Hydrol.* 212–213, 36–50.
- Lindroth, A., 1985. Seasonal and diurnal variation of energy budget components in coniferous forests. *J. Hydrol.* 82, 1–15.
- Mizutani, K., Ikeda, T., 1994. Evaporation of intercepted rainfall from a *Castanopsis cuspidata* Schottky forest using various micrometeorological methods. Proceedings of the International Symposium on Forest Hydrology, Tokyo, Japan, 99 pp. 69–76.
- Pearce, A.J., Rowe, L.K., 1981. Rainfall interception in a multi-storied, evergreen mixed forest: estimates using Gash's analytical model. *J. Hydrol.* 49, 342–353.
- Rutter, A.J., Kershwa, K.A., Robins, P.C., Morton, A.J., 1971. A predictive model of rainfall interception in forests. I. Derivation of the model from observations in a plantation of Corsican pine. *Agric. Meteorol.* 9, 367–384.
- Rutter, A.J., Morton, A.J., Robins, P.C., 1975. A predictive model of rainfall interception in forests. II. Generalization of the model and comparison with observations in some coniferous and hardwood stands. *J. Appl. Ecol.* 12, 367–380.
- Schulze, R.E., Scott-Shaw, C.R., Nanni, U.W., 1978. Interception by *Pinus patula* in relation to rainfall parameters. *J. Hydrol.* 36, 393–396.
- Stewart, J.B., 1977. Evaporation from the wet canopy of a pine forest. *Water Resour. Res.* 13, 915–921.
- Tsukamoto, Y., Ohta, T., Minemura, T., 1988. Rainfall interception during rains. Proceedings of 1988 Annual Conference. *Jpn Soc. Hydrol. Water Resour.*, Tokyo, 40–41 in Japanese.

- Yoshida, H., Hashino, M., 1994. A methodology for estimating forest evaporation by a rainfall interception tank model based on stemflow data. , Proceedings of the International Symposium on Forest Hydrology, Tokyo, Japan pp. 47–54.
- Yoshida, H., Hashino, M., Muraoka, K., 1993. A method of estimating forest rainfall interception by tank model based on stem flow data. J. Jpn Soc. Hydrol. Water Resour. 6, 19–30 in Japanese, with English Abstract.
- Yulianur, A., Yoshida, H., Hashino, M., 1998. The estimation of rainfall interception loss using Hamon's potential evapotranspiration and linear regression. J. Jpn. Soc. Hydrol. Water Resour. 11, 141–149 in Japanese, with English Abstract.